water

Article

Using Stable Water Isotopes to Analyze Spatiotemporal Variability and Hydrometeorological Forcing in Mountain Valley Wetlands

Julia M. Hathaway [1], Richard M. Petrone [1,*], Cherie J. Westbrook [2], Rebecca C. Rooney [3] and Lindsey E. Langs [4,5]

[1] Department of Geography and Environmental Management, University of Waterloo, 200 University Avenue West, Waterloo, ON N2L 3G1, Canada; jhathaway@uwaterloo.ca
[2] Department of Geography and Planning, University of Saskatchewan, 117 Science Place, Saskatoon, SK S7N 5C8, Canada; cherie.westbrook@usask.ca
[3] Department of Biology, University of Waterloo, 200 University Avenue West, Waterloo, ON N2L 3G1, Canada; rebecca.rooney@uwaterloo.ca
[4] Center for Hydrology, University of Saskatchewan, Saskatoon, AB S7N 3H5, Canada; lindsey.langs@usask.ca
[5] Hydrometeorology Research Group, Department of Geography and Environmental Management, University of Waterloo, Waterloo, ON N2L 3G1, Canada
* Correspondence: rich.petrone@uwaterloo.ca; Tel.: +1-519-888-4567

Abstract: Wetlands in Montane and Subalpine Subregions are increasingly recognized as important hydrologic features that support ecosystem function. However, it is currently not clear how climate trends will impact wetland hydrological processes (e.g., evaporative fluxes) across spatiotemporal scales. Therefore, identifying the factors that influence wetland hydrologic response to climate change is an important step in understanding the sensitivity of these ecosystems to environmental change. We used stable water isotopes of hydrogen and oxygen (δ^2H and δ^{18}O), coupled with climate data, to determine the spatiotemporal variability in isotopic signatures of wetland source waters and understand the influence of evaporative fluxes on wetlands in the Kananaskis Valley. Our results show that the primary runoff generation mechanism changes throughout the growing season resulting in considerable mixing in wetland surface waters. We found that evaporative fluxes increased with decreasing elevation and that isotopic values became further removed from meteoric water lines during the late peak- and into the post-growing seasons. These findings suggest that a change in the water balance in favor of enhanced evaporation (due to a warmer and longer summer season than present) will not only lead to greater water loss from the wetlands themselves but may also reduce the water inputs from their catchments.

Keywords: subalpine; montane; isotopes; evaporation; wetlands; Rocky Mountains; runoff; deuterium excess

Citation: Hathaway, J.M.; Petrone, R.M.; Westbrook, C.J.; Rooney, R.C.; Langs, L.E. Using Stable Water Isotopes to Analyze Spatiotemporal Variability and Hydrometeorological Forcing in Mountain Valley Wetlands. *Water* **2022**, *14*, 1815. https://doi.org/10.3390/w14111815

Academic Editor: Maurizio Barbieri

Received: 28 April 2022
Accepted: 29 May 2022
Published: 5 June 2022

1. Introduction

Mountain wetlands are considered to play an important role in regional hydrologic processes that underlie a range of potential ecosystem services. Perhaps some of the most valuable are flood attenuation, water storage, carbon abatement, biodiversity support, and their ability to import and export materials (e.g., sediment, organic matter, nutrients, etc.) [1]. Anthropogenic climate change is expected to significantly alter hydrologic regimes in montane and subalpine environments, potentially affecting the ability of wetlands to perform these key services [2]. For instance, studies report decreases in the duration of snow cover and a reduction in snowpack water content, concurrent with observed increases in air temperatures [3,4], which could potentially create periods of drought or low flow in mountain wetlands. Moreover, earlier extreme rain events during spring are shown to quicken snowmelt, leading to the rapid onset of flood events (e.g., Pomeroy et al. [5]).

These observations, coupled with the ecological importance of wetlands in intermountain regions, provide the motivation to better understand how hydroclimate processes effect wetland functions.

Stable water isotopes of hydrogen and oxygen (δ^2H and δ^{18}O), and Deuterium Excess (d-excess), in combination with climate data, provide a useful and increasingly applied method for integrating hydrological process information, and identifying spatiotemporal patterns [6]. D-excess in precipitation, as defined by Daansgard, [7], is mainly related to climatic conditions (temperature, relative humidity, and wind speed) at moisture source regions and is widely used to trace moisture sources and recycling [8]. Moisture evaporated from land surface is formed by plant transpiration and evaporation of water from soils, lakes, and wetlands [9]. The latter component is high in d-excess as a result of kinetic isotope fractionation during evaporation. Recycling of such moisture to the atmosphere increases the d-excess of the atmospheric vapor and consequently of the precipitation formed by condensation of this vapor. Thus, the systematic differences in d-excess signals in various water sources/types within watersheds generally reflect the significance of evaporation loss in the water balance of hydrological components [10].

Craig [11] established that seasonal and climatically driven interactions between the δ^2H and δ^{18}O content of water in precipitation results in a Local Meteoric Water Line (LMWL), which can be linked to water sources to assess the relative importance of seasonal precipitation contribution to regional surface waters [12]. Linear deviations from the LMWL, referred to as the Local Evaporation Line (LEL), are a result of evaporation of surface water that enriches the heavy oxygen and hydrogen content of the remaining water [13]. The LEL can be used to provide basin-scale estimates of the degree of evapotranspiration (ET) and water inflow to individual water bodies [12,14]. The slope of the LEL reflects the influence of varying local conditions (temperature, relative humidity, wind speed, etc.) naturally integrated over the evaporative season [15]. Relative displacement along the LEL for a given evaporation rate is also characteristic of local conditions, as is the limiting enrichment [15]. The application of stable isotope end-members, in combination with climate data, will contribute to the understanding of the hydrologic processes that support wetlands, and provide insights into the implications of continued environmental change [16].

Numerous researchers have investigated source water dynamics using an isotopic approach and identified spatiotemporal variations in source water isotopic signatures and their meteorological conditions [8,17–19]. Semwal et al. [20] identified the isotopic composition of waters and vapor sources using isotopic measurements in Sukhna Lake in the Himalayan foothills. Marchina et al. [21] used water isotopes as spatiotemporal tracers to identify headwater origins in the Italian Alps. Shi et al. [22] used stable water isotopes to investigate the isotopic signature of surface waters in the Yellow River of the Tibetan Plateau, and better understand the cycling of hydrogen and oxygen isotopes in the regional water cycle. Wu et al. [23] used stable water isotopes to investigate the geographic and environmental variables that influence the isotopic composition of river water across Kazakhstan. Cao et al. [24] investigated the origin of different source waters within the Caohai Wetland catchment in the northwestern Guizhou Province. Biggs et al. [25] used an isotope evaporation model to determine the fraction of evaporated inflow to high elevation lakes. Several regional studies employed isotopes to evaluate orographic effects on precipitation and altitude effects on source water isotopic composition [26–30].

The leeward slopes of the Canadian Rocky Mountains support an abundance of wetland ecosystems [31], making them an excellent location to study wetland hydrological processes. Often referred to as the “water tower” of Canada, the water resources of the Canadian Rocky Mountains are highly important for drinking water, agricultural uses, and natural habitat [6,32]. Estimations of how hydroclimatic variations will impact wetland source water trends in the south-eastern Canadian Rocky Mountains are important, however, few studies have addressed this due to the physical challenges presented by the rugged landscapes and remote location. Combining new and historical datasets, this study seeks to investigate spatiotemporal patterns in wetland source waters using stable isotopes of hydrogen and oxygen (δ^2H and $\delta^{18}O$), and assess relevant hydrometric controls throughout the Kananaskis Valley, Alberta, Canada. The objectives of this paper are to: (I) understand the influence of evaporative fluxes on extensive wetland sites across an elevation range, and (II) determine the spatial and temporal variability in intensive wetland source waters (e.g., groundwater, rain, snow, stream, and surface water) over multiple seasons, and the factors influencing them (e.g., climate controls and elevation).

2. Materials and Methods

2.1. Study Site Description

Data for this research was collected throughout a ~1981 km^2 area in the eastern region of the Canadian Rockies, all located within 50 km of Calgary, Alberta. Sites were located in the Kananaskis River Valley (50°46′43.14″ N, 115°20′32.89″ W), part of the Stoney-Nakoda First Nations reserve, and three municipal districts. The study area ranges in elevation from 1280 to 1980 m a.s.l., with the highest elevation wetlands located in Peter Lougheed Provincial Park (Figure 1). The study area forms the western margin of the Western Canada sedimentary basin and is therefore geologically complex [6]. Strata (sandstone, limestone, shale, and dolomite) are folded and faulted, ranging in age from Cambrian to Cretaceous [33], and are covered by glacial, lacustrine, and fluvial materials [34]. The mountain region is characterized by glaciated U-shaped valleys, with moraines at higher elevations and valleys dissected by rivers at lower elevations. Land use activities in the area are restricted with uses such as forest harvesting permitted in the Improvement Districts but not in Provincial Parks. Land use in alpine regions includes recreational hiking, camping, and skiing, while lower elevation regions are characterized by a rolling topography and more varied uses, such as recreational vehicles and equestrian activity.

The climate of the Kananaskis Valley is subject to spatiotemporal variation due to orographic influence. Precipitation follows a continental pattern and is heaviest in June and July. It varies from 400 to 550 mm annually, with potential evapotranspiration in the same range, making the area semi-arid [33]. The closest Environment and Climate Change Canada (ECCC) weather station (ID 3053600) with 30+ years of climate records is located in the north-eastern margin of the study area (51.01° N, 115.03° W) at an elevation of 1391 m a.s.l. The warmest month, July, is 14.1 °C on average, while the coldest month, January, has a mean temperature of −7.5 °C. Although, temperatures are quite variable with extremes of 33.9 °C and −45.6 °C. Weather changes are largely controlled by disturbances in the circumpolar westerlies that allow for continuous movement of airmasses through the region [35]. During the winter months, climate is controlled by two major airmasses: the Pacific airmass and Arctic airmass that develop over Siberia and the Arctic Ocean, respectively. In the Kananaskis region, Chinook winds commonly occur during winter months and can affect the local climate and hydrology due to their warm and dry conditions [35]. During the early summer months, the Kananaskis Valley receives limited sunlight as a result of low temperatures that bring cloudy, moist air to the region. During the growing season, Chinook winds create low night-time relative humidity that is largely independent of vegetation cover, site, and topography [11]. At higher elevations in the valley, the majority of annual precipitation occurs as snow or a mixture of rain and snow with the greatest snow depths in the upper bands of elevation.

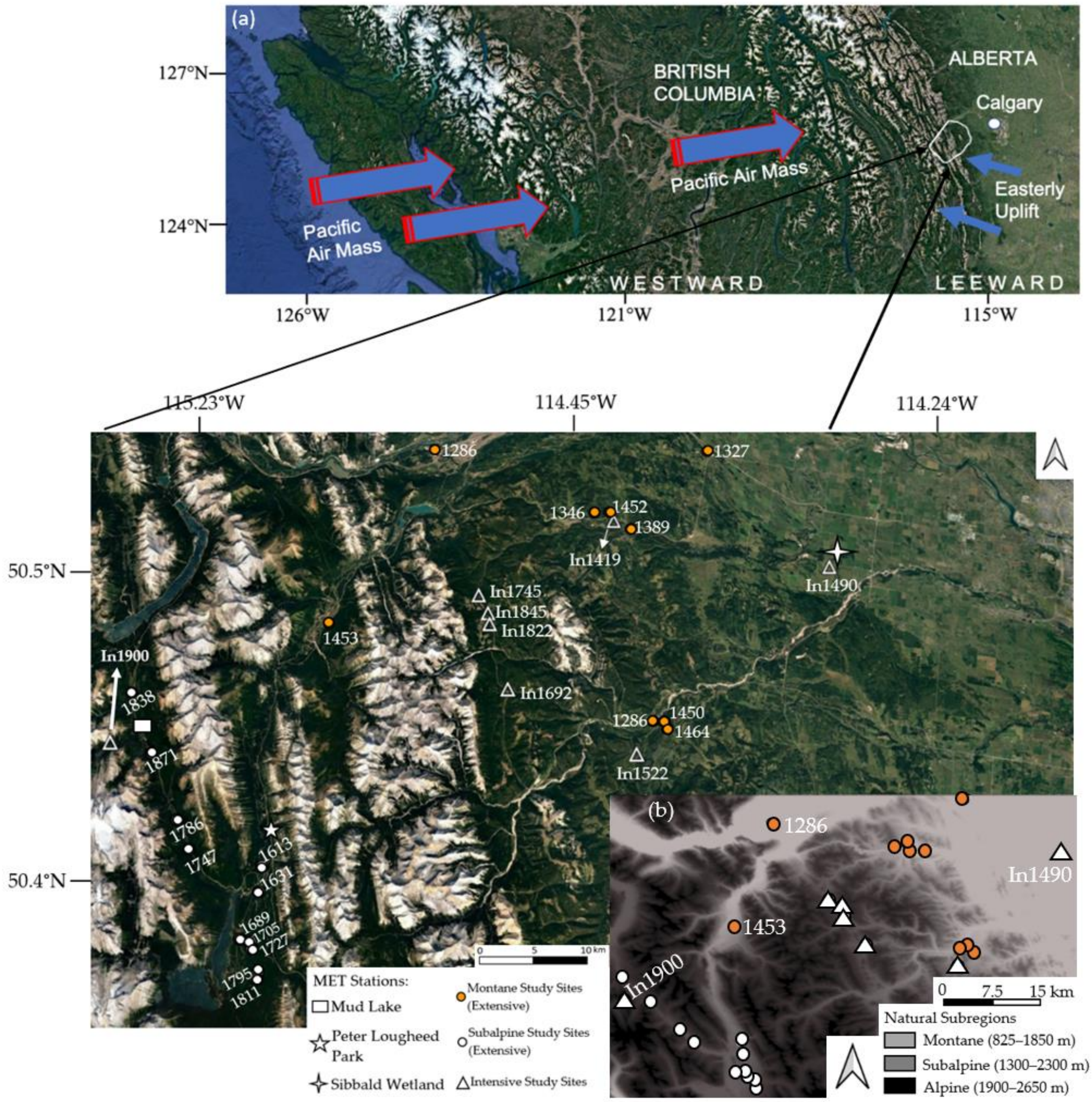

Figure 1. Site map illustrating isotope sampling and MET station locations. Extensive sites in the Montane Natural Subregion are shown in orange circles (n = 9) and sites in the Subalpine Natural Subregion are shown by white circles (n = 11) with black outline. Intensive sites are depicted by white triangles (n = 8). The white arrows point to site label. The surrounding area from Calgary (East) to the Pacific Ocean including influential air masses from the Pacific Ocean and Easterlies from the Gulf of Mexico is shown in (**a**). Study site is shown by the white outline. Classic orographic effects occur on the westward side resulting in rain out of heavier isotopes at low elevations (shown). Mixing of pacific air mass and easterlies occur on the leeward side. Digital Elevation Map of the study site using geospatial data from Government of Canada shown in (**b**). Natural Subregions of Interest are depicted by color.

2.2. Wetland Identification

Eight intensive wetlands, at different elevations, were studied during the 2018, 2019, and 2020 growing seasons. Intensive wetlands were established in 2018 and each site was equipped with a groundwater monitoring well and precipitation bucket to collect groundwater and rain water samples for isotopic analysis. The number associated with each identifier is the elevation in m a.s.l. of the specific wetland.

In 2012, 529 wetland sites were established by Morrison et al. [6] to assess peatland distribution and beaver habitat. Original inventorying of extensive wetlands involved general analysis of aerial imagery in 2007 and 2008. In 2012, a subset of 90 wetland sites from the original 529 sites was selected for isotopic sampling of beaver pond water; no other wetland source waters were sampled at extensive sites.

For the purpose of this study, a smaller subset of 20 sites (extensive) was randomly selected from the previous 90 sites, then divided into Natural Subregions; Upper Foothills, Montane, or Subalpine as shown in Figure 1. The sampled wetlands' elevation ranged from 1286 m a.s.l. to 1971 m a.s.l., intersecting the elevation ranges of Upper Foothills, Montane, and Subalpine Natural Subregions; 950–1750 m a.s.l., 825–1850 m a.s.l., and 1300–2300 m a.s.l., respectively [36]. From this point forward, the Upper Foothills and Montane were grouped and referred to as the Montane Natural Subregion since both Natural Subregions are directly below the Subalpine Natural Subregion depending on their location in respect to the Bow River [37].

The Montane Natural Subregion covers 1.3% of the province that ranges in elevation from 825–1850 m a.s.l. [36]. The temperatures range from −10.0 °C to 13.9 °C and there is 589 mm of mean annual precipitation [36]. The habitat contains grasslands and mixed or aspen (*Populus* species), lodgepole pine (*Pinus Contorta*), Douglas fir (*Pseudotsuga menziesii*), and white spruce forests (*Picea glauca*) [36].

The Subalpine Natural Subregion covers 3.8% of the province that ranges in elevation from 1300–2300 m a.s.l. [36]. In the Upper Bow River Basin, this Natural Subregion occurs above the Montane or Foothills Natural Subregion depending on the location [36]. North of the Bow River, the Subalpine is above the Upper Foothills Natural Subregion and south of the Bow River, the Subalpine is above the Montane Natural Subregion. In this study, no sites intercept with the Foothills Natural Subregion. The temperature of the Subalpine Subregion ranges from −11.7 °C to 11.3 °C and has 755 mm of mean annual precipitation [36]. The habitat contains mixed conifer forests of lodgepole pine (*Pinus Contorta)* and Engelmann spruce (*Picea engelmannii*) [36].

2.3. Isotope Data Collection

Surface water samples for isotopic analysis were collected from beaver ponds at extensive sites (n = 20) in 2012, during the pre- and peak-growing season (June–July) by Morrison et al. [6]. Surface water samples for isotopic analysis was repeated in the post-growing season (August-September) of 2022. Samples were collected in ponds with low water movement. Surface sample collection at intensive sites (n = 8) occurred during 2018 and 2019 throughout the growing season at sites with sufficient standing water. Intensive sites were then sampled again during September of 2020. Detailed collection methods are described in Hathaway et al. [38]. In brief, water samples were bottled with minimal headspace and stored at room temperature (never refrigerated or frozen to limit phase changing) before processing. The temporal record, and number of samples collected at each site, is summarized in Table S1.

Groundwater was sampled from a repeat well location during the snowmelt period starting in May, through the late growing season period in September at intensive sites in 2019. The groundwater table was consistently at the surface during the pre- and peak-growing seasons. However, the water table fell below the well depth (one meter) during the end of the peak-growing season and into the post growing season at several of the intensive sites.

Rain sample collection began at the end of the peak-growing season in 2018 at intensive sites when collectors were installed. In 2019, rain was measured monthly throughout the growing season (May–September) when there were precipitation events. Rain collectors were only available at two sites (In1900 and In1419) during the 2020 sampling campaign.

Snow samples were only collected for pre- and post-growing season sampling periods due to availability during 2018 and 2019. Snow was collected any time it was present, which was usually in spring during snowmelt or fall when accumulation was starting.

Stream samples were collected throughout the 2018 and 2019 growing seasons (May–September) at intensive sites with flowing streams. All 2020 stream samples were collected late in the growing season again due to restricted access to sampling sites.

All water samples collected in 2018, 2019, and 2020 were processed and analyzed at the Environmental Isotope Laboratory (EIL) at the University of Waterloo, Waterloo, Ontario. Samples were processed with the $\delta^{18}O$ and $\delta^{2}H$ LGR-OA-ICOS Laser System using methods as described by the EIL, University of Waterloo (LGR, 2010; Berman et al., 2013). Maximum analytical uncertainties are $\pm$ 0.1‰ for $\delta^{18}O$ and $\pm$ 2‰ for $\delta^{2}H$. Quality control was maintained by running a range of water standards including VSMOW (Vienna Standard Mean Ocean Water) and VSLAP (Vienna Standard Light Antarctic Precipitation) from the International Atomic Energy Agency (IAEA). Duplicates were run at a minimum of every fifth samples. Each run also included an in-house check standard for QA/QC of each individual sample batch. Electric conductivity was assumed to be in normal range due to past measurements in the area. Samples collected in 2012 were analyzed at the McDonnell Hillslope Hydrology Lab at the University of Saskatchewan using the same equipment and methods described above.

2.4. Meteorological Data

Meteorological (MET) data, including temperature and precipitation (Figure 2), were used from three separate stations, each shown in Figure 1. Mud Lake data was collected by instrumentation on a tripod positioned 4.15 m above the ground near site In1900. MET data included relative humidity and temperature measured with a HMP 155 (Vaisala, Finland), as well as rainfall. Rain precipitation was measured at Mud Lake at 2.03 m above ground using an Ott Pluvio 400 (Ott Hydromet, Loveland, CO, USA). The Peter Lougheed Park station is located at 1622 m a.s.l. and is operated by Alberta Sustainable Resource Development. The Sibbald meteorological station is positioned at 1490 m a.s.l. and is equipped with a Rotronic HC2-S3 probe to measure air temperature and a Texas Electronics TE525 tipping bucket to measure rainfall. This MET station is part of the Canadian Rockies Hydrological Observatory.

2.5. Data Analysis

D-excess was calculated as $\delta D = \delta^{2}H - 8 \times \delta^{18}O$ [8]. D-excess is associated with kinetic fractionation, which is typically indicative of evaporation or condensation [19], and can be thought of as an index of deviation from the Global Meteoric Water Line (GMWL), which has a d-excess value of 10‰ [13]. Rain samples with d-excess < 10 fall below the GMWL and have experienced water loss by evaporation. In addition, due to the close relationship between $\delta^{18}O$ and δD in precipitation, values can reflect different environmental characteristics in precipitation moisture sources. Thus, d-excess was used in this study to interpret evaporative and non-evaporative signals across the landscape, and identify meteorological factors associated with different moisture sources throughout the growing season.

Weighted means were calculated for rain and d-excess for the 2018 and 2019 growing seasons using,

$$\delta_{\mathrm{WA}} = \Sigma(P_{\mathrm{i}} \cdot \delta_{\mathrm{i}}) / \Sigma P \quad (1)$$

where δ_{i} is the measured isotopic value during the precipitation event and P_{i} is precipitation (mm) during that period [39]. Rain samples were collected monthly from intensive sites for isotopic analysis, and precipitation data was used from Mud Lake and Kananaskis Valley meteorological stations. Since samples were collected monthly at all sites, values were averaged to get an estimate of rain signals for the region. Precipitation data was totaled for each month to determine the cumulative amount for the collection period.

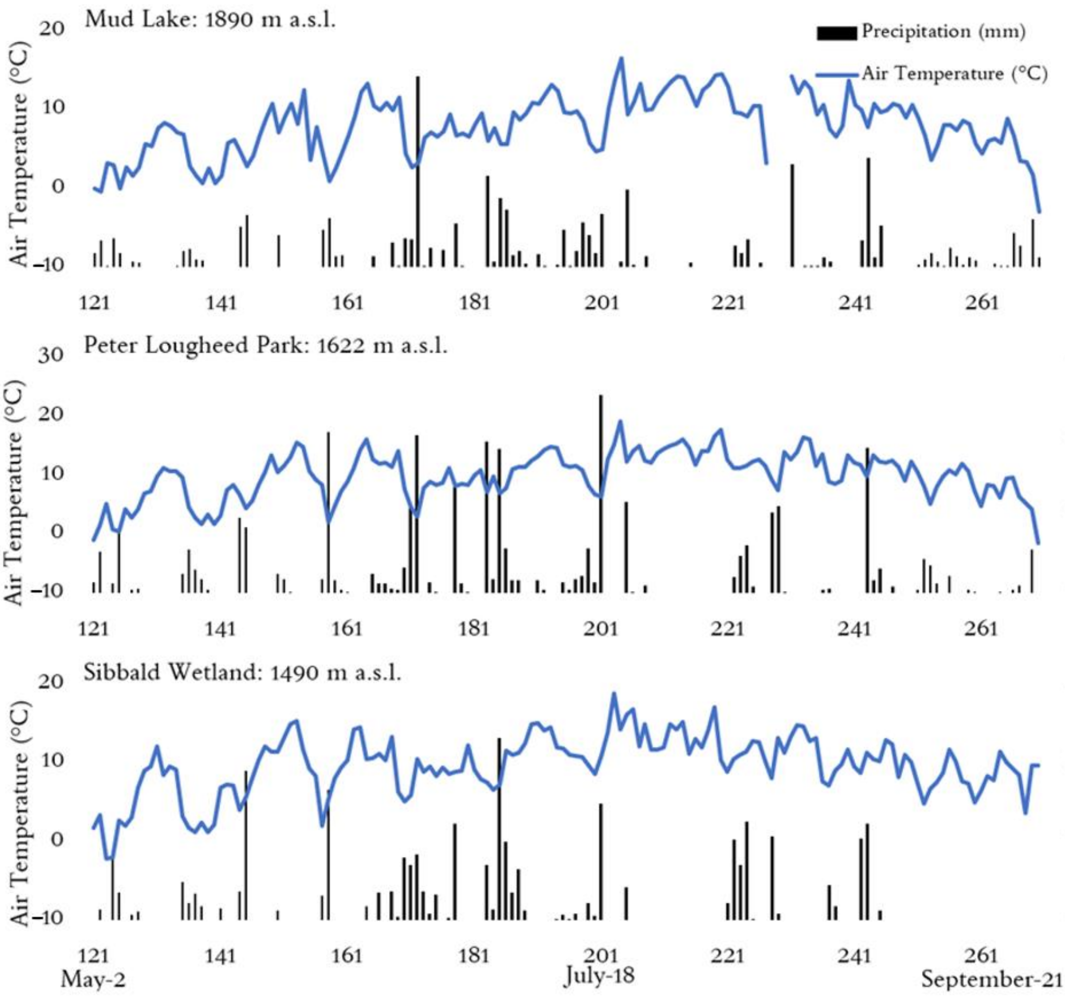

Figure 2. Basic meteorological conditions including precipitation and air temperature from Mud Lake, Peter Lougheed Park, and Sibbald Wetland, Kananaskis, Alberta. Shown are the 2019 daily averages from 1 May to 27 September 2019.

3. Results

3.1. Spatial Variability in Isotopes

The spatiotemporal data of Oxygen-18 values in source waters from intensive sites over the three growing seasons showed a typical annual cycle (Figure 3). Rain samples were isotopically enriched with a median of −17.8‰ and plotted outside the values of groundwater, stream, and surface water. Snow samples were significantly more depleted with a median of −23.5‰, however, they were widely distributed, thus providing a strong tracer for glacial melt versus snowmelt (Figure 3). Groundwater, stream, and surface water values were clustered between rain and snow with median values of −19.05‰, −19‰, −19.4‰, respectively. This clustering pattern indicates a degree of infiltration and mixing of rain and snow with surface, stream, and groundwater to a depth of at least one meter where groundwater samples were collected. The slope of the regression line for all water sources was lower than that of the LMWL on the order of 7.18 (snow) > 7.01 (groundwater), 7.00 (rain) > 6.71 (surface) > 5.45 (stream), indicating evaporative fractionation for all sources. Surface water values plotted across the GMWL, LMWL, and LEL, which may be associated with contrasting water sources and increased residence times in surface waters versus streams (see source plots, Figure 4). Interestingly, the isotopic results do not show a clear-cut, linear relationship in which the hydrogen and oxygen heavy isotopes of rainwater decrease with increasing altitude. Instead, we see a slight depletion in $\delta^{18}O$ near the transition zone between the Subalpine and Montane Subregions before becoming enriched again in the subalpine range. The exact causation of these results is complicated since the precipitation processes on the leeward slopes of the Rockies are heavily influenced by the mixing of air masses and highly variable due to interactions between ambient flow and topography.

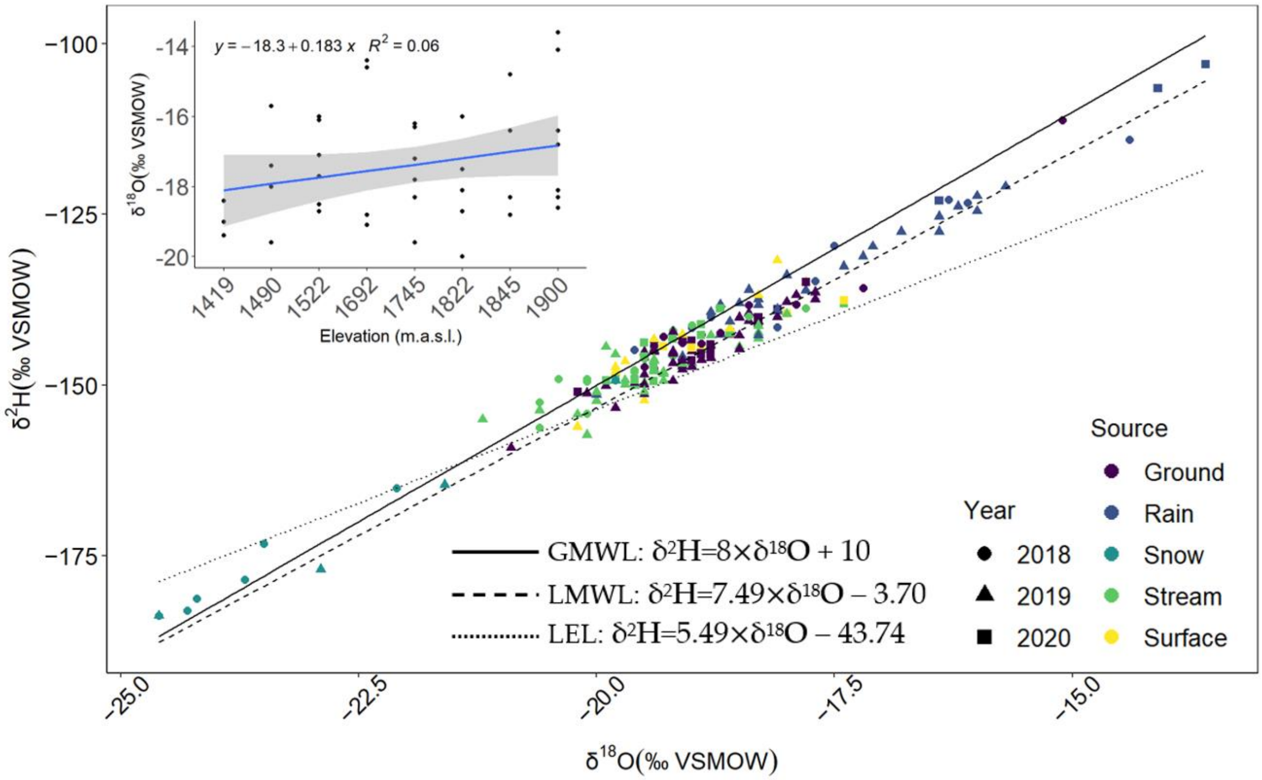

Figure 3. Dual isotope plot, with the source depicted by color, of grouped groundwater, rain, snow, stream, surface water samples collected at intensive sites in 2018, 2019, 2020 plotted along the GMWL. LMWL and LEL taken from Katvala et al. [40] for the Kananaskis Valley, Alberta, Canada. Inset figure is a plot of rain δ^{18}O vs. elevation (increasing elevation from right to left) shown for all rain data.

Samples from the subalpine wetland (In 1900) trended more towards the GMWL, despite having a lower slope, indicating greater influence of meteoric water sources (Figure 4). Between groundwater, stream, and surface water samples at intensive sites, stream values were the most depleted in δ^{18}O. There was a distinct clustering pattern of isotopically depleted stream samples originating from site In1900, potentially indicating the importance of snow and glacial melt as a component of stream flow generation.

Mid-altitude wetlands (1692–1845 m a.s.l.) had the largest distribution of δ^{18}O values with a minimum of −24.2‰ and maximum of −14.8‰, which is expected for this region [41] (Figure 4). Observed groundwater, stream, and surface water values plot close together and remain relatively uniform despite minor fluctuations and slight δ^{18}O enrichment in subalpine regions (Figure 4). As for δ^{18}O in wetland pond water at extensive sites, values were overall more widely distributed with a range of −6.5‰ and a median of −18.02‰ (Figure 5). The slope of the Subalpine Subregion regression line (4.53) was slightly lower than the Montane Subregion regression line (4.77), however, both slopes were similar to that of the LEL and the majority of points plot along the LEL, which is associated with evaporation in both regions. Partial evaporation from open surface water suggests that residual surface waters were enriched and the evaporated moisture was depleted in the heavy isotopes of Hydrogen and Oxygen, thus following the evaporation line instead of the GMWL (Figure 5). Moreover, d-excess values for all samples plotted below 10‰, the global average d-excess, indicating further evaporative influence at all wetland sites (Figure 6).

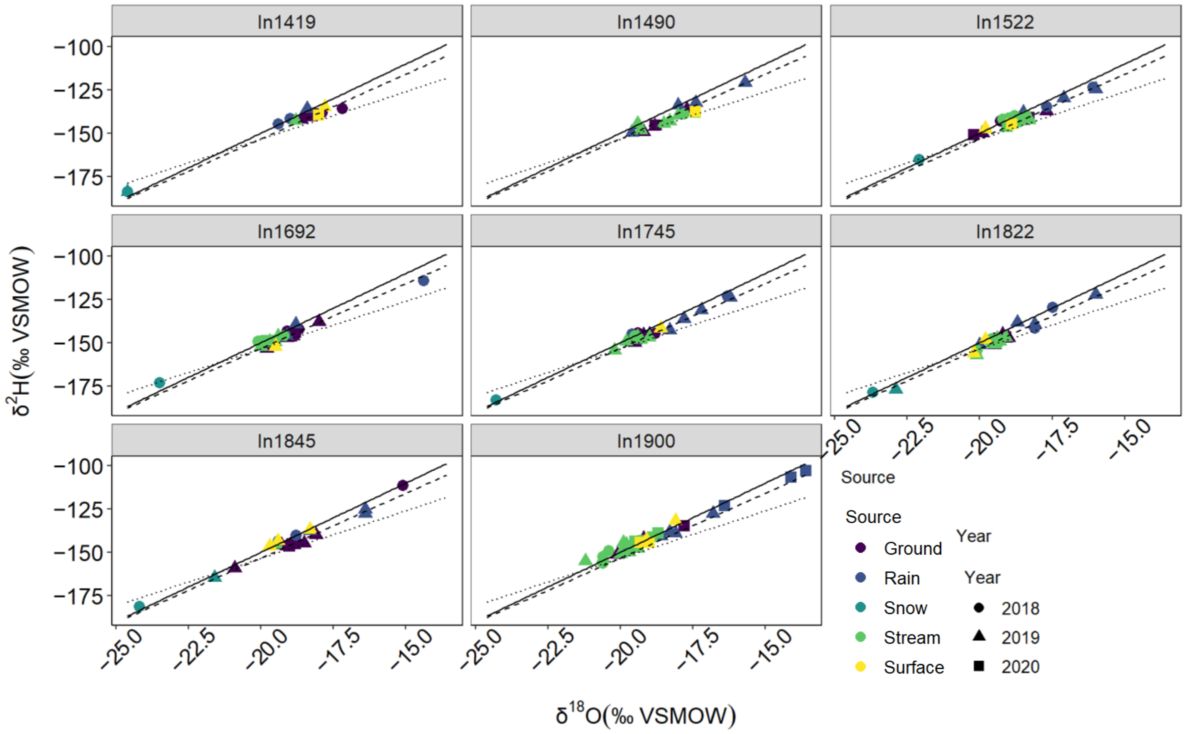

Figure 4. Dual Isotope plot grouping all source waters by color and year by shape for individual intensive sites (n = 8). Global Meteoric Water Line ($\delta^2H - 8 \times \delta^{18}O + 10$), Local Meteoric Water Line ($\delta^2H - 7.488 \times \delta^{18}O - 3.7$), and Local Evaporation Lines ($\delta^2H = 5.498 \times \delta^{18}O - 43.74$) are shown as solid, dashed and dotted lines, respectively. The local evaporation lines are for the Kananaskis Valley, Alberta.

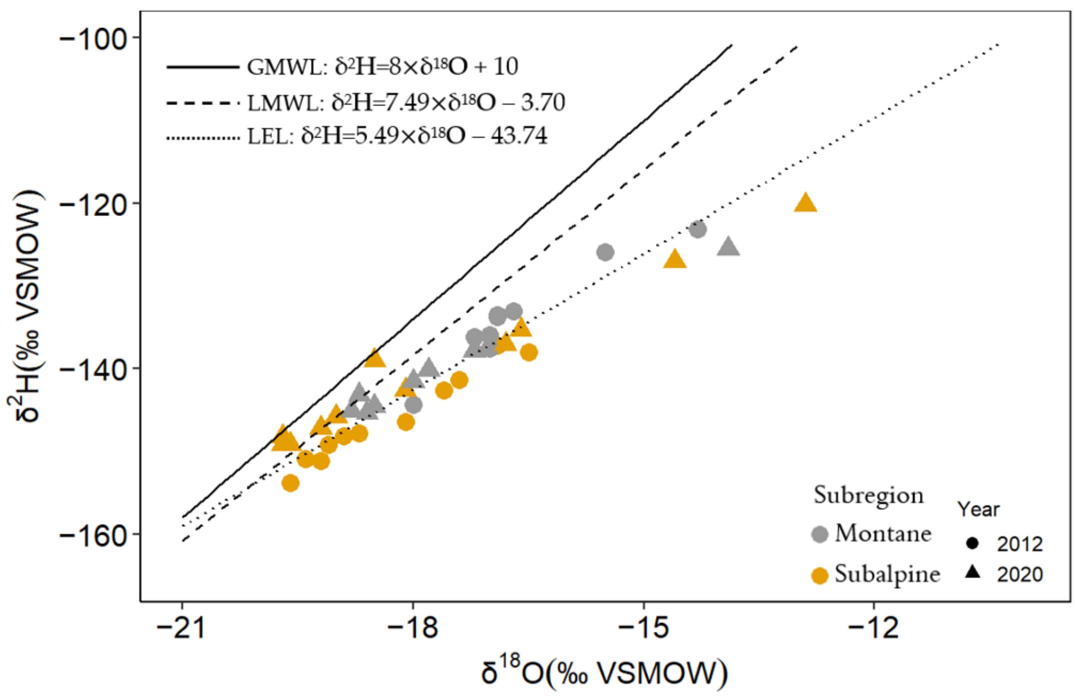

Figure 5. Dual isotope plot of surface water samples collected from beaver ponds at extensive sites during the 2012 growing season (June–July) and 2020 peak- and post-growing season (August–September). Natural Subregion of Interest is depicted by color and year is depicted by shape. LMWL and LEL taken from Katvala et al. [40] for the Kananaskis Valley, Alberta.

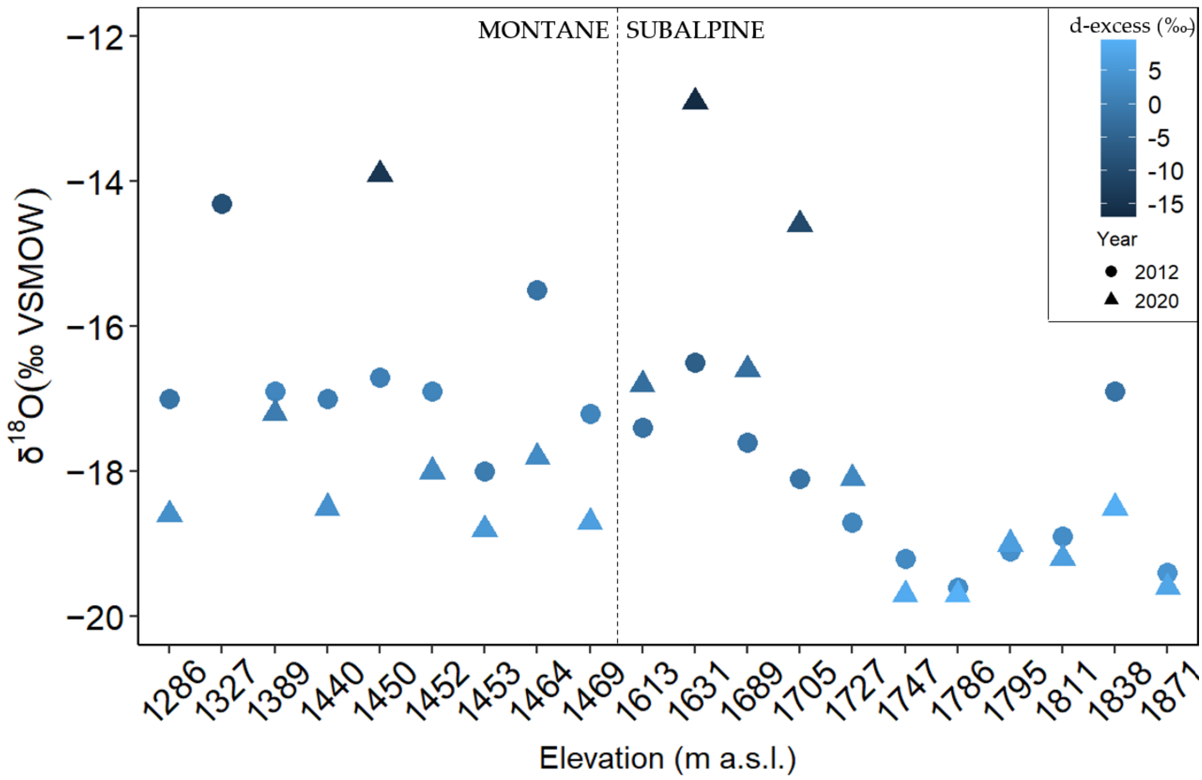

Figure 6. $\delta^{18}O$ and d-excess values shown for extensive wetland pond surface water samples across the Montane and Subalpine Natural Subregions. Year is depicted by symbol shape and, d-excess is depicted by color.

The distribution of $\delta^{18}O$ values from the Subalpine Subregion were greater compared to the Montane Subregion, however, the Subalpine Subregion average was more isotopically depleted (−18‰, −17.1‰, respectively). There was a slightly more pronounced linear altitude-isotope relationship among Extensive site surface waters, with values becoming more isotopically depleted as altitude increased, correlated with increasing d-excess for both 2012 (R^2 0.28) and 2020 (R^2 0.11) (Figure 6). Correlations between $\delta^{18}O$, d-excess, and elevation were used to test the influence of geographic variables on surface water isotopic values for 2012 and 2020. Positive correlations were found between $\delta^{18}O$ values and elevation for 2012 (Figure 6). However, despite a slightly stronger altitude–isotope gradient, 2020 data showed a weak, negative correlation that was not significant at $p < 0.05$ (Figure 6).

3.2. *Temporal Variability in Isotopes*

Spatiotemporal data for $\delta^{18}O$ values in groundwater, rain, snow, stream, and surface water from intensive sites over the three growing seasons are shown in Figure 7. Source water data showed a typical annual cycle with depleted winter/spring values and enriched summer values (Figure 7). This annual cycle is best demonstrated during the 2019 growing season due to the completeness of the dataset, in which source waters become more enriched, following seasonal rain precipitation events (Figure 2). Groundwater showed the highest temporal variability followed by surface water and streams. Interestingly, stream water was consistently more depleted than groundwater at all sites (Figure 7). Within site In1900, the distribution of $\delta^{18}O$ groundwater signals was much greater at the end of the growing season relative to lower elevation sites, which could be caused by inputs from different water sources (e.g., glacial melt, upslope runoff). D-excess was used in this study to assess evaporation effects in the landscape and identify moisture sources for precipitation. Results show strong seasonality with high d-excess values occurring during the peak-post growing seasons and low values during pre-growing season (Figure 7).

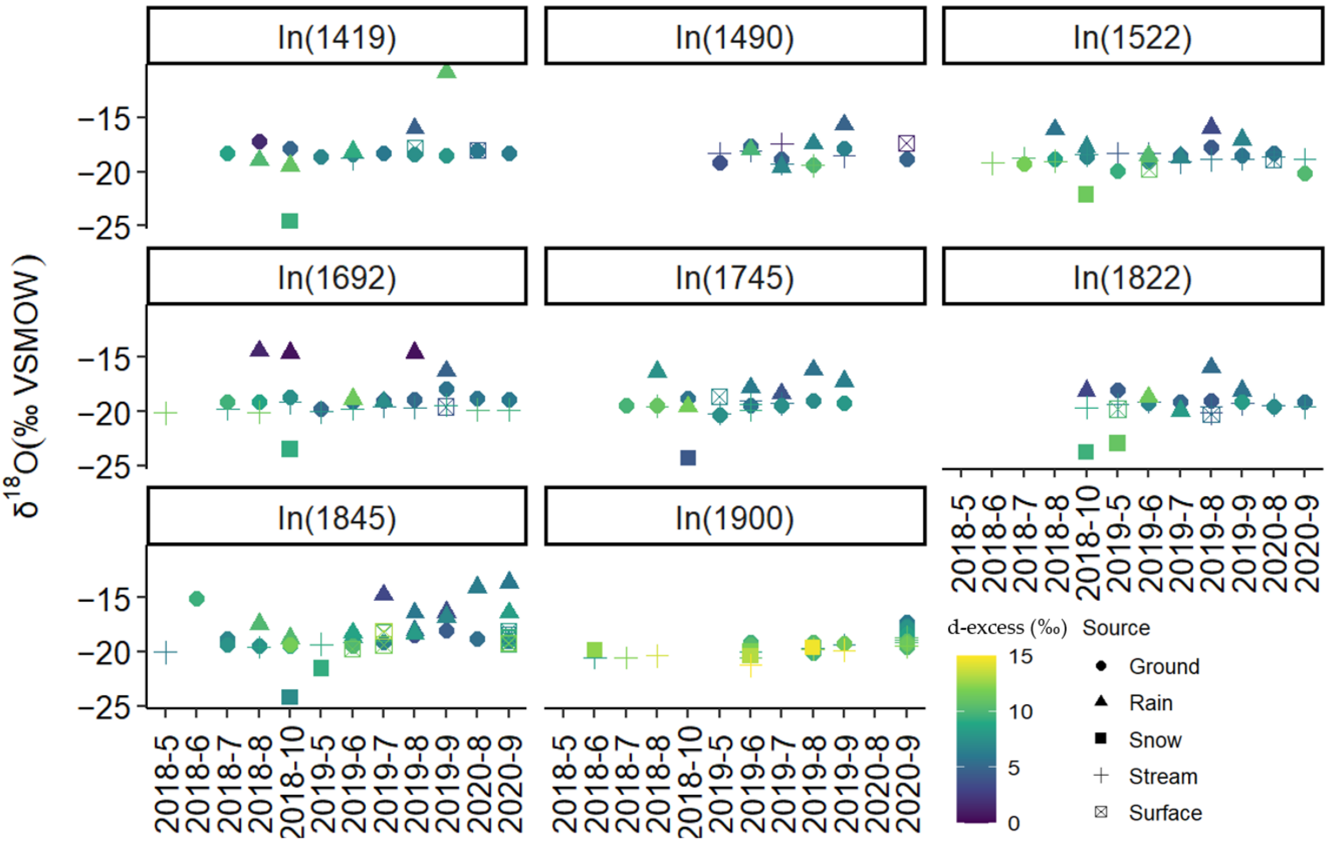

Figure 7. Spatiotemporal plot of $\delta^{18}O$ and d-excess for all intensive sites throughout the 2018 and 2019 growing seasons. D-excess is depicted by color and source waters are distinguished by symbol for groundwater, rain, snow, stream, and surface water.

Not surprisingly, d-excess did not show strong seasonality within individual sites, but did increase with rising elevation (Figure 7). Site In1900 had the highest d-excess values, with two source averages plotting above the global average (stream (10.1‰), and snow (13.5‰)) (Figure 7). This site experiences minimal evaporative influence, indicating that the enriched $\delta^{18}O$ values are potentially a result of environmental characteristics and not evaporative fractionation.

The growing season weighted average of precipitation d-excess calculated from intensive data for the study region is 7.27‰ (2019) and 8.34‰ (2018), which is below the average d-excess of the global meteoric water (Figure 8). In general, the median d-excess value of snow was the highest (11.21, 8.34‰), followed by stream (9.51, 7.25‰), surface (NA, 9.49‰), and groundwater (8.60, 6.87‰) for 2018 and 2019, respectively. Most importantly, the median d-excess of groundwater plotted below the median of precipitation d-excess in 2019 during pre-, peak-, and post growing seasons, indicating continued evaporative influence throughout the growing season. Although the d-excess median of groundwater plotted above the median of precipitation d-excess in 2018, there were values that plotted below 7.27‰, however, these derived from Montane sites primarily during the peak-post growing season (Figure 7).

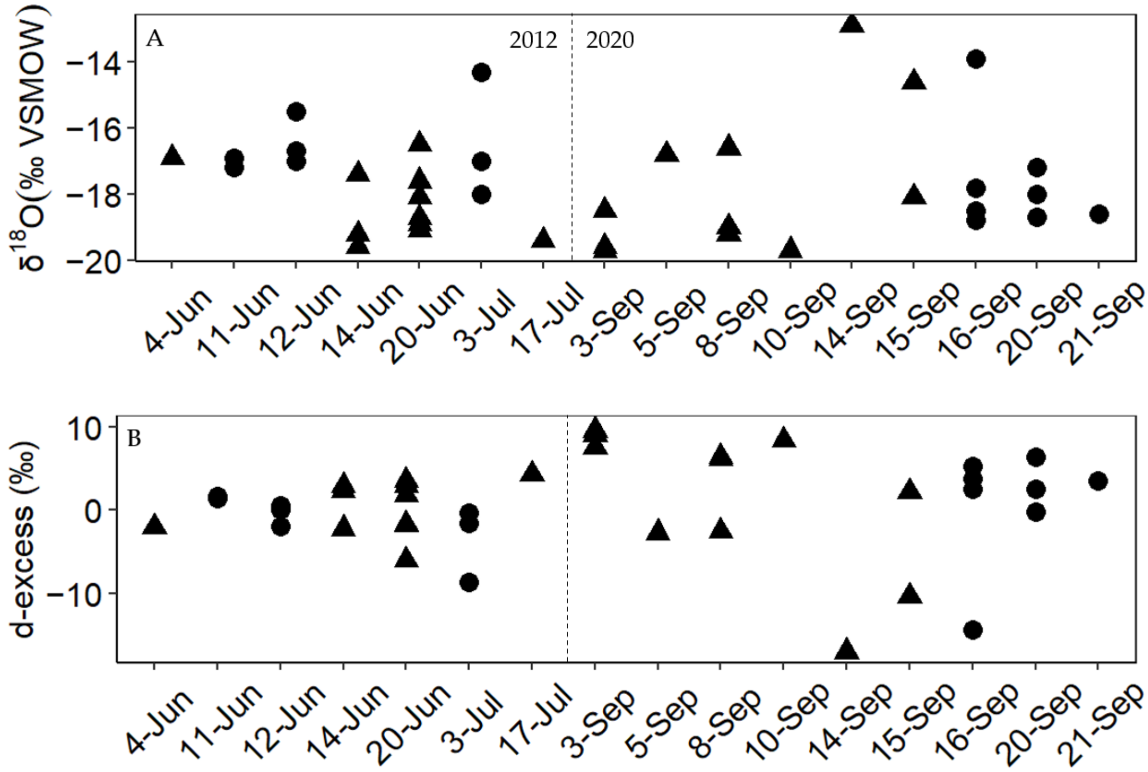

Figure 8. Time-series distribution of δ^{18}O (**A**) and d-excess (**B**) values from extensive sites for each sampling period in 2012 and 2020. Natural Subregions are depicted by shape for clarity. The Montane Natural Subregion is represented by circles and the Subalpine Natural Subregion is represented by triangles.

The distribution of δ^{18}O data from surface waters at extensive sites showed progressively more variation throughout the growing season, especially from the Subalpine Subregion, and depleted average δ^{18}O values for the snowmelt period that remained relatively depleted through the peak 2012 growing season (Figure 8). The δ^{18}O composition of surface water from Montane sites showed relatively damped variability, which could be due to the gap in data between the pre- and post-growing seasons. We would expect enrichment of δ^{18}O during the peak-growing season correlated with increased temperatures and precipitation. The average δ^{18}O value during the pre-peak growing seasons was −17.41‰ (±1.17) and post growing season was −17.5‰ (±1.6). In 2020, samples collected during the post-growing season generally appeared to be more depleted in δ^{18}O, except at subalpine sites, where δ^{18}O values remained between −18.5‰ and −19.5‰, indicating mixed moisture sources and precipitation inputs (Figure 8).

4. Discussion

Mountain wetland ecosystems are expected to be among the most sensitive to changing climate as their persistence depends on factors directly influenced by climate (e.g., precipitation, snowpack, evaporation). Despite their importance and sensitivity, such processes tend to be understudied due to the difficulty of data collection in rugged mountain landscapes. This research addressed the hydroclimate processes that control wetland function, and how they affect wetland source water composition across spatiotemporal scales. We used stable water isotopes and climate data to investigate evaporative influence on wetland surface waters and determine spatiotemporal trends in isotopic signatures in montane and subalpine wetlands. This research is important as climate patterns in montane regions are changing, and it is currently not clear how hydroclimate controls will affect wetland dynamics. Overall, evaporative fluxes from wetland source waters followed the expected seasonal trend, exhibiting stronger evaporative signals during the summer associated with high temperatures and longer sun exposure. Consistent with Hathaway et al. [38], isotopic signals indicate mixing between source waters within individual intensive wetlands, demonstrating water derivation from both rain and snow at different times throughout the growing season.

4.1. Spatial Variability in Isotopes

Groundwater, rain, snow, stream, and surface water data from intensive sites showed a normal δ^{18}O distribution, with enriched rain and depleted snow signatures, consistent with global patterns [19,23,42]. Minimal variability of isotopes in groundwater, stream, and surface waters, compared to rain and snow indicates the mixing of snowmelt/rainfall throughout the growing season with stored water in the landscape. Comparing the hydrogen and oxygen isotopes of groundwater and stream water with the LMWL, we see that the stream water and groundwater points are located at the upper left of the LMWL and are close to the atmospheric precipitation line. This indicates that precipitation has a replenishing effect on stream water and groundwater, especially during the late summer. This pattern is consistent with results from Semwal et al. [21], in which the similarities between groundwater signatures and the LMWL were used to demonstrate the importance of rainfall as a recharge source in the Himalayan foothills. The observed increase in d-excess and δ^{18}O depletion in high elevation streams (1800–1900 m a.s.l.), was also reported in Leuthold et al. [43], and is likely the result of a high snow to rain precipitation ratio and the effects of cool, short summers on meteorological conditions [44]. The more enriched δ^{18}O median in streams (-18.8‰) and groundwater (-18.5‰) at low elevations could indicate preferential sourcing of stream water from isotopically heavier rain, longer groundwater residence times allowing for rain infiltration from the surface, and/or water enriched by evaporation from storage in wetland landscape [19]. The overall more enriched δ^{18}O median of groundwater (-19.00‰) compared to streams (-19.75‰) is the result of evaporative influence confirmed by higher d-excess in streams (10.55‰), as compared to groundwater (6.5‰).

The observed ambiguous δ^{18}O-elevation gradient of rain is likely due to temporally complex, local climate conditions on the leeward side of the Canadian Rocky Mountains. In lee-slope environments, the δ^{18}O-elevation relationship often reflects the patterns of moisture transport and deposition and is significantly altered by processes such as subcloud evaporation and mixing of different air masses [41,45]. Under specific circumstances such processes can create an ambiguous or inverse δ^{18}O-elevation relationship, whereby δ^{18}O becomes more enriched with increasing elevation. In a meta-analysis by Poage and Chamberlain [46] of observed δ^{18}O-elevation gradients from 68 different studies worldwide, all but two studies reported δ^{18}O depletion with altitude, one of which was within the eastern Canadian Rocky Mountains. Kong and Pang [45] reported similar findings as a result of inverse orographic effects, at a comparable latitude (46° N) and elevation range, in a semi-arid alpine setting in the Tianshan Mountains of Northwest China. In the Canadian Rocky Mountains, inverse δ^{18}O-elevation gradients specifically occur when easterly systems from the Gulf of Mexico bring rainfall from continued rainout of air masses as they span topographic barriers [44]. Then, continued Rayleigh fractionation distillation (removal of δ^{18}O from cloud) occurs as systems are pushed upwards, which creates a reverse orographic effect [41]. Since the results from this study do not show a strong linear δ^{18}O-elevation relationship (R^2 0.0076), there is likely mixing of Pacific air masses and continental weather originating from the southeast, creating the ambivalent results [47].

Surface waters in mountain landscapes are subject to a variety of environmental factors that influence their isotopic composition [48]. The specific focus on wetland ponds (extensive sites) in this study is unique and provides an opportunity to evaluate hydrometeorological influence and hydrologic connectivity in wetland abundant landscapes. The range of isotopic signatures of subalpine wetlands was greater than those of the Montane Subregion, likely due to the overlap in Natural Subregion elevation ranges, and therefore characteristics of subalpine versus montane wetlands. For example, a greater presence of open grasslands in the Montane Subregion promotes evaporation from surface waters driving more enriched δ^{18}O signals. This is evident in Figure 5 as the majority of data from Montane sites trend along the LEL. The higher end of the subalpine range is dominated by forested landscapes and more commonly exhibits complex terrain, interfering with sunlight. Our results demonstrate this effect as d-excess drops off at higher elevations. Shade effects are clearly shown in Hrach et al. [32], in which a shaded subalpine wetland received significantly less sunlight throughout the growing season compared to an unobstructed site.

4.2. Temporal Variability in Isotopes

Temporal analysis of stable water isotope data from intensive sites aligns with studies that seek to map patterns of δ^{18}O and d-excess in wetlands and other surface waters [2,19,22,41,49]. Similar to temporal patterns described by Ala-aho et al. [19] in a low elevation, cold region climate, all sites showed suppressed variability of source water signals within individual sites, but slight enrichment from the pre- to post-growing season. δ^{18}O in streams was slightly more depleted during snowmelt (May) (-19.99‰ $\pm$ 0.6) than the peak-growing season (July and August) (-19.35‰ $\pm$ 0.7). There was not steady linear enrichment of δ^{18}O throughout the peak- and post-seasons, providing evidence of a longer snowmelt period, close proximity to depleted groundwater reserves, and/or minimal evaporative influence. The general seasonal similarities between δ^{18}O content of streams and groundwater, which is documented in wetlands, shows that groundwater that supports wetland function is supplied by inflows from stream water as well as from rainfall [50]. Observed δ^{18}O enrichment of stream water during the peak- and post-growing seasons could be explained by evaporative fractionation as shown by decreasing d-excess values, increased rainfall inputs, or greater mixing due to reliance on groundwater for stream flow generation.

The overall temporal isotopic analysis of δ^{18}O and d-excess in wetland surface waters at extensive sites were highly variable, and the exact causation is difficult to discern. During the 2012 pre-growing season, both Montane and Subalpine sites follow an expected distribution with δ^{18}O values decreasing from June to July. The temperature profiles from the Subalpine versus Montane field site are similar during this period, however, fluctuations throughout the growing season are not as severe at the Montane site, and temperatures are overall more mild. These conditions could explain the more depleted δ^{18}O signatures from the Montane sites. During late June and into early July, surface waters became significantly more depleted in δ^{18}O coupled with increased d-excess, especially at high elevations. This is likely the result of a later and prolonged snowmelt at sites in the Subalpine region and a combination of higher temperatures and rainfall in the Montane region. During the peak growing season, the damped variation in d-excess is likely from persistent inputs of snowmelt and rain water, minimizing evaporation from surface waters. Similar studies documented δ^{18}O enrichment in surface waters in alpine and subalpine regions during the peak-growing season, coupled with decreased d-excess values, indicating that the distribution of samples along the LEL are likely the result of a combined precipitation inputs and evaporative effects due to prolonged residence times [42,50]. Moreover, d-excess values of stream and groundwater from intensive sites have a higher average than surface waters throughout the growing season, again indicating poor connectivity between wetlands, and minimal mixing between surface waters and other water inputs. A possible explanation for stunted hydrologic connectivity is the documented effects of beaver populations on hydrologic flow paths. Beaver dams are known to temporally change water storage and connectivity in the eastern Canadian Rocky Mountains [51]. However, this requires further research to determine the extent of beaver influence on connectivity and its effect on d-excess.

4.3. Limitations and Future Work

Glacial meltwater was not sampled in this study, however, the importance of glacial meltwater to groundwater recharge during the late summer in mountain valleys is well documented [52,53]. Due to the absence of glacial meltwater isotopic data, insights into the source water mixing within wetland surface waters was limited. Moreover, the quantity of snow samples collected in this study were sparse and only represented the latter portion of the pre-growing season. The relatively enriched signals of snow during the pre-growing season are likely the result of progressive seasonal isotopic enrichment that snowpacks undergo during the melting process [54].

The improved conceptual understanding of evaporative fluxes and runoff generation gained from this study is an important framework that can be tested with modeling to provide insights into the future response of wetland ecosystems to changing hydrological processes in the Canadian Rocky Mountains. Future modeling efforts should focus on quantifying water loss due to evaporation from wetland surfaces during the peak- and post-growing seasons. We also suggest future work should continue to use stable water isotopes to determine the relative importance of glacial meltwater to wetlands in the Montane and Subalpine Subregions. These efforts will help water resource managers and land managers best prepare for adverse effects due to climate change and other anthropogenic activities.

5. Conclusions

This study investigated spatiotemporal patterns of hydrogen and oxygen (δ^2H and δ^{18}O) in wetland source waters, and assessed relevant hydrometric controls throughout the Kananaskis Valley, Alberta, Canada. Based on our results, we hypothesize that the primary runoff generation mechanism changes throughout the growing season. During the pre-growing season, snowmelt water is readily mobilized to streams, then during the peak-growing season, stored water in the landscape is displaced and becomes the dominant driver of hydrologic connectivity between mountain streams. Under this scenario, a change in the water balance in favor of enhanced evaporation (due to warmer and longer summer seasons than present) would not only lead to greater water loss from wetlands themselves, but may also reduce the water inputs from their catchments. This is unfavorable to most existing wetlands, and in extreme scenarios may result in drying of wetlands in Montane and Subalpine regions. As indicated by the variations in isotopic signatures from wetlands in the Montane versus Subalpine regions, individual ecosystems will be adversely affected. The insights gained from this study contribute to our overall understanding of mountain wetland hydrology and can be applied to future studies that seek to quantify evaporation loss and source water dynamics in Montane and Subalpine environments.

Supplementary Materials: The following supporting information can be downloaded at: https://www.mdpi.com/article/10.3390/w14111815/s1, Table S1. Summary of samples collected from intensive sites from years 2018–2020 throughout the growing season (May–October). The number and type of sample collected at each site during each month is shown.

Author Contributions: Conceptualization, R.M.P. and J.M.H.; methodology, R.M.P., J.M.H., C.J.W. and R.C.R.; software, J.M.H.; validation, J.M.H., C.J.W., R.C.R. and L.E.L.; formal analysis, J.M.H.; investigation, J.M.H. and R.M.P.; writing—original draft preparation, J.M.H.; writing—review and editing, R.M.P., C.J.W., R.C.R. and L.E.L.; visualization, J.M.H., C.J.W. and R.C.R.; supervision, R.M.P.; project administration, R.M.P.; funding acquisition, R.M.P. All authors have read and agreed to the published version of the manuscript.

Funding: This research received no external funding.

Institutional Review Board Statement: Not applicable.

Informed Consent Statement: Not applicable.

Data Availability Statement: The data presented in this study are available on request from the corresponding author.

Acknowledgments: We would like to thank our funding partners, Canada First Research Excellence Fund, Global Water Futures, Mountain Water Futures Program, Alberta Innovates, and Natural Science and Engineering Research Council of Canada Discovery and CREATE grants programs for the financial support on research conducted within this project. Thank you to Sheryl Chau and Yi

Abby Wang for their assistance in data collection during the summers of 2019 and 2020. Finally, thank you to Matt Bolding, Calvin Lei, and Jordan Reynolds from the Rooney Lab (University of Waterloo) for conducting the vegetation survey and sharing raw data and Alasdair Morrison and Jeff Kardas for collection of water samples for isotope analysis in 2012. This research was funded by Canada First Research Excellence Fund under Global Water Futures; Canadian Natural Science and Engineering Research Council of Canada CREATE Program in Water Security.

Conflicts of Interest: The authors declare no conflict of interest.

References

1. Kadykalo, A.N.; Findlay, C.S. The flow regulation services of wetlands. *Ecosyst. Serv.* **2016**, *20*, 91–103. [CrossRef]
2. Brooks, J.R.; Mushet, D.M.; Vanderhoof, M.K.; Leibowitz, S.G.; Christensen, J.R.; Neff, B.P.; Rosenberry, D.O.; Rugh, W.D.; Alexander, L.C. Estimating wetland connectivity to streams in the Prairie Pothole Region: An isotopic and remote sensing approach. *Water Resour. Res.* **2018**, *54*, 955–977. [CrossRef] [PubMed]
3. Rangwala, I.; Miller, J.R. Climate change in mountains: A review of elevation-dependent warming and its possible causes. *Clim. Chang.* **2012**, *114*, 527–547. [CrossRef]
4. Stewart, I.T. Changes in snowpack and snowmelt runoff for key mountain regions. *Hydrol. Processes Int. J.* **2009**, *23*, 78–94. [CrossRef]
5. Pomeroy, J.W.; Stewart, R.E.; Whitfield, P.H. The 2013 flood event in the South Saskatchewan and Elk River basins: Causes, assessment and damages. *Can. Water Resour. J. Rev. Can. Des Ressour. Hydr.* **2016**, *41*, 105–117. [CrossRef]
6. McDonnell, J.J.; Beven, K. Debates—The future of hydrological sciences: A (common) path forward? A call to action aimed at understanding velocities, celerities and residence time distributions of the headwater hydrograph. *Water Resour. Res.* **2014**, *50*, 5342–5350. [CrossRef]
7. Dansgaard, W. Stable isotopes in precipitation. *Tellus* **1964**, *16*, 436–468. [CrossRef]
8. Cui, J.; Tian, L.; Biggs, T.W.; Wen, R. Deuterium-excess determination of evaporation to inflow ratios of an alpine lake: Implications for water balance and modeling. *Hydrol. Processes* **2017**, *31*, 1034–1046. [CrossRef]
9. Froehlich, K.; Kralik, M.; Papesch, W.; Rank, D.; Scheifinger, H.; Stichler, W. Deuterium excess in precipitation of Alpine regions–moisture recycling. *Isot. Environ. Health Stud.* **2008**, *44*, 61–70. [CrossRef]
10. Whitfield, P.H. Climate station analysis and fitness for purpose assessment of 3053600 Kananaskis, Alberta. *Atmos. Ocean* **2014**, *52*, 363–383. [CrossRef]
11. Craig, H. Standard for reporting concentrations of deuterium and oxygen-18 in natural waters. *Science* **1961**, *133*, 1833–1834. [CrossRef] [PubMed]
12. Wassenaar, L.I.; Athanasopoulos, P.; Hendry, M.J. Isotope hydrology of precipitation, surface and ground waters in the Okanagan Valley, British Columbia, Canada. *J. Hydrol.* **2011**, *411*, 37–48. [CrossRef]
13. Craig, H.; Gordon, L.I. *Deuterium and Oxygen 18 Variations in the Ocean and the Marine Atmosphere, in Stable Isotopes in Oceanographic Studies and Palaeotemperatures, Spoleto 1965*; Tongiorgi, E., Ed.; Consiglio Nazionale della Richerche: Pisa, Italy, 1965; pp. 9–130.
14. Gat, J.R. Oxygen and hydrogen isotopes in the hydrologic cycle. *Annu. Rev. Earth Planet. Sci.* **1996**, *24*, 225–262. [CrossRef]
15. Gibson, J.J.; Edwards, T.W.D.; Bursey, G.G.; Prowse, T.D. Estimating Evaporation Using Stable Isotopes: Quantitative Results and Sensitivity Analysis for Two Catchments in Northern Canada: Paper presented at the 9th Northern Res. Basin Symposium/Workshop (Whitehorse/Dawson/Inuvik, Canada-August 1992). *Hydrol. Res.* **1993**, *24*, 79–94. [CrossRef]
16. Penna, D.; Engel, M.; Mao, L.; Dell'Agnese, A.; Bertoldi, G.; Comiti, F. Tracer-based analysis of spatial and temporal variations of water sources in a glacierized catchment. *Hydrol. Earth Syst. Sci.* **2014**, *18*, 5271–5288. [CrossRef]
17. Carol, E.; Braga, F.; Da Lio, C.; Kruse, E.; Tosi, L. Environmental isotopes applied to the evaluation and quantification of evaporation processes in wetlands: A case study in the Ajó Coastal Plain wetland, Argentina. *Environ. Earth Sci.* **2015**, *74*, 5839–5847. [CrossRef]
18. Ala-Aho, P.; Soulsby, C.; Pokrovsky, O.S.; Kirpotin, S.N.; Karlsson, J.; Serikova, S.; Vorobyev, S.N.; Manasypov, R.M.; Loiko, S.; Tetzlaff, D. Using stable isotopes to assess surface water source dynamics and hydrological connectivity in a high-latitude wetland and permafrost influenced landscape. *J. Hydrol.* **2018**, *556*, 279–293. [CrossRef]
19. Shi, Y.; Jia, W.; Zhu, G.; Ding, D.; Yuan, R.; Xu, X.; Zhang, Z.; Yang, L.; Xiong, H. Hydrogen and Oxygen Isotope Characteristics of Water and the Recharge Sources in Subalpine of Qilian Mountains, China. *Pol. J. Environ. Stud.* **2021**, *30*, 2325–2339. [CrossRef]
20. Semwal, P.; Khobragarde, S.; Joshi, S.K.; Kumar, S. Variation in δ^{18}O and δ^{2}H values of rainfall, surface water, and groundwater in the Sukhna Lake basin in northwest India. *Environ. Earth Sci.* **2020**, *79*, 1–14. [CrossRef]
21. Marchina, C.; Lencioni, V.; Paoli, F.; Rizzo, M.; Bianchini, G. Headwaters' isotopic signature as a tracer of stream origins and climatic anomalies: Evidence from the Italian Alps in summer 2018. *Water* **2020**, *12*, 390. [CrossRef]
22. Shi, M.; Wang, S.; Argiriou, A.A.; Zhang, M.; Guo, R.; Jiao, R.; Kong, J.; Zhang, Y.; Qiu, X.; Zhou, S. Stable Isotope Composition in Surface Water in the Upper Yellow River in Northwest China. *Water* **2019**, *11*, 967. [CrossRef]
23. Wu, H.; Wu, J.; Song, F.; Abuduwaili, J.; Saparov, A.S.; Chen, X.; Shen, B. Spatial distribution and controlling factors of surface water stable isotope values (δ^{18}O and δ^{2}H) across Kazakhstan, Central Asia. *Sci. Total Environ.* **2019**, *678*, 53–61. [CrossRef] [PubMed]

24. Cao, X.; Wu, P.; Zhou, S.; Han, Z.; Tu, H.; Zhang, S. Seasonal variability of oxygen and hydrogen isotopes in a wetland system of the Yunnan-Guizhou Plateau, southwest China: A quantitative assessment of groundwater inflow fluxes. *Hydrogeol. J.* **2018**, *26*, 215–231. [CrossRef]
25. Biggs, T.W.; Lai, C.T.; Chandan, P.; Lee, R.M.; Messina, A.; Lesher, R.S.; Khatoon, N. Evaporative fractions and elevation effects on stable isotopes of high elevation lakes and streams in arid western Himalaya. *J. Hydrol.* **2015**, *522*, 239–249. [CrossRef]
26. Kumar, U.S.; Kumar, B.; Rai, S.P.; Sharma, S. Stable isotope ratios in precipitation and their relationship with meteorological conditions in the Kumaon Himalayas, India. *J. Hydrol.* **2010**, *391*, 1–8. [CrossRef]
27. Gonfiantini, R.; Roche, M.A.; Olivry, J.C.; Fontes, J.C.; Zuppi, G.M. The altitude effect on the isotopic composition of tropical rains. *Chem. Geol.* **2001**, *181*, 147–167. [CrossRef]
28. Mezga, K.; Urbanc, J.; Cerar, S. The isotope altitude effect reflected in groundwater: A case study from Slovenia. *Isot. Environ. Health Stud.* **2014**, *50*, 33–51. [CrossRef]
29. Giustini, F.; Brilli, M.; Patera, A. Mapping oxygen stable isotopes of precipitation in Italy. *J. Hydrol. Reg. Stud.* **2016**, *8*, 162–181. [CrossRef]
30. Xu, Q.; Hoke, G.D.; Liu-Zeng, J.; Ding, L.; Wang, W.; Yang, Y. Stable isotopes of surface water across the L ongmenshan margin of the eastern T ibetan P lateau. Geochemistry, Geophysics. *Geosystems* **2014**, *15*, 3416–3429.
31. Morrison, A.; Westbrook, C.J.; Bedard-Haughn, A. Distribution of Canadian Rocky Mountain wetlands impacted by beaver. *Wetlands* **2015**, *35*, 95–104. [CrossRef]
32. Hrach, D.M.; Petrone, R.M.; Van Huizen, B.; Green, A.; Khomik, M. The Impact of Variable Horizon Shade on the Growing Season Energy Budget of a Subalpine Headwater Wetland. *Atmosphere* **2021**, *12*, 1473. [CrossRef]
33. Toop, D.C.; de la Cruz, N.N. *Hydrogeology of the Canmore Corridor and Northwestern Kananaskis Country, Alberta*; Report to Western Economic Partnership Agreement; Western Economic Diversification Canada, Alberta Environment, Hydrogeology Section: Edmonton, AB, Canada, 2002.
34. Gignac, L.D.; Vitt, D.H.; Zoltai, S.C.; Bayley, S.E. Bryophyte response surfaces along climatic, chemical, and physical gradients in peatlands of western Canada. *Nova Hedwig.* **1991**, *53*, 27–71.
35. Harder, P. *Hydroclimatological Trends in the Kananaskis Valley. Centre for Hydrology Internal Report*; University of Saskatchewan: Saskatoon, SK, Canada, 2008.
36. Downing, D.J.; Pettapiece, W.W. *Natural regions and subregions of Alberta*; Government of Alberta: Stony Plain, AB, Canada, 2006; Pub. No.T/852.
37. Reynolds, J.N.; Swanson, H.K.; Rooney, R.C. Habitat area and environmental filters determine avian richness along an elevation gradient in mountain peatlands. *J. Avian Biol.* **2022**, *2*, e02797. [CrossRef]
38. Hathaway, J.M.; Westbrook, C.; Rooney, R.C.; Petrone, R.M.; Langs, L.L. Quantifying relative contributions of source waters from a subalpine wetland to downstream water bodies. *Hydrol. Processes* **2022**, in review.
39. Yang, Q.; Mu, H.; Guo, J.; Bao, X.; Martín, J.D. Temperature and rainfall amount effects on hydrogen and oxygen stable isotope in precipitation. *Quat. Int.* **2019**, *519*, 25–31. [CrossRef]
40. Katvala, S.M. Isotope hydrology of the upper Bow River basin. Master's Thesis, University of Calgary, Calgary, AB, Canada, 2008.
41. Moran, T.A.; Marshall, S.J.; Evans, E.C.; Sinclair, K.E. Altitudinal gradients of stable isotopes in lee-slope precipitation in the Canadian Rocky Mountains. *Arct. Antarct. Alp. Res.* **2007**, *39*, 455–467. [CrossRef]
42. Tazioli, A.; Cervi, F.; Doveri, M.; Mussi, M.; Deiana, M.; Ronchetti, F. Estimating the isotopic altitude gradient for hydrogeological studies in mountainous areas: Are the low-yield springs suitable? insights from the Northern Apennines of Italy. *Water* **2019**, *11*, 1764. [CrossRef]
43. Leuthold, S.J.; Ewing, S.A.; Payn, R.A.; Miller, F.R.; Custer, S.G. Seasonal connections between meteoric water and streamflow generation along a mountain headwater stream. *Hydrol. Processes* **2021**, *35*, e14029. [CrossRef]
44. Thériault, J.M.; Hung, I.; Vaquer, P.; Stewart, R.E.; Pomeroy, J.W. Precipitation characteristics and associated weather conditions on the eastern slopes of the Canadian Rockies during March–April 2015. *Hydrol. Earth Syst. Sci.* **2018**, *22*, 4491–4512. [CrossRef]
45. Kong, Y.; Pang, Z. A positive altitude gradient of isotopes in the precipitation over the Tianshan Mountains: Effects of moisture recycling and sub-cloud evaporation. *J. Hydrol.* **2016**, *542*, 222–230. [CrossRef]
46. Poage, M.A.; Chamberlain, C.P. Empirical relationships between elevation and the stable isotope composition of precipitation and surface waters: Considerations for studies of paleoelevation change. *Am. J. Sci.* **2001**, *301*, 1–15. [CrossRef]
47. Smith, C.D. The relationship between monthly precipitation and elevation in the Alberta foothills during the foothills orographic precipitation experiment. In *Cold Region Atmospheric and Hydrologic Studies. The Mackenzie GEWEX Experience*; Springer: Berlin/Heidelberg, Germany, 2008; pp. 167–185.
48. Kendall, C.; Coplen, T.B. Distribution of oxygen-18 and deuterium in river waters across the United States. *Hydrol. Processes* **2001**, *15*, 1363–1393. [CrossRef]
49. Flaim, G.; Camin, F.; Tonon, A.; Obertegger, U. Stable isotopes of lakes and precipitation along an altitudinal gradient in the Eastern Alps. *Biogeochemistry* **2013**, *116*, 187–198. [CrossRef]
50. Carol, E.; del Pilar Alvarez, M.; Candanedo, I.; Saavedra, S.; Arcia, M.; Franco, A. Surface water–groundwater interactions in the Matusagaratí wetland, Panama. *Wetl. Ecol. Manag.* **2020**, *28*, 971–982. [CrossRef]
51. Ronnquist, A.L.; Westbrook, C.J. Beaver dams: How structure, flow state, and landscape setting regulate water storage and release. *Sci. Total Environ.* **2021**, *785*, 147333. [CrossRef]

52. Fang, X.; Pomeroy, J.W. Diagnosis of future changes in hydrology for a Canadian Rockies headwater basin. *Hydrol. Earth Syst. Sci.* **2020**, *24*, 2731–2754. [CrossRef]
53. Taylor, S.; Feng, X.; Kirchner, J.W.; Osterhuber, R.; Klaue, B.; Renshaw, C.E. Isotopic evolution of a seasonal snowpack and its melt. *Water Resour. Res.* **2001**, *37*, 759–769. [CrossRef]
54. Woo, M.K.; Young, K.L. High Arctic wetlands: Their occurrence, hydrological characteristics and sustainability. *J. Hydrol.* **2006**, *320*, 432–450. [CrossRef]